Femtosecond dynamics of photocyclization of 1-[(4-{5-[4-chloromethyl-2,5-dimethyl-3-thienyl]-2-oxo-1,3-dioxol-4-yl}-2,5-dimethyl-3-thienyl)methyl]pyridinium chloride

S. M. Aldoshin,[a] E. A. Yur´eva,[a] N. A. Sanina,[a] M. M. Krayushkin,[b] D. V. Tsyganov,[b] F. E. Gostev,[c] I. V. Shelaev,[c] O. M. Sarkisov,[c] and V. A. Nadtochenko[a]*

[a] *Institute of Problems of Chemical Physics, Russian Academy of Sciences, 1 prosp. Akad. Semenova, 142432 Chernogolovka, Moscow Region, Russian Federation. Fax: +7 (495) 522 3507. E-mail: yurieva@icp.ac.ru*

[b] *N. D. Zelinsky Institute of Organic Chemistry, Russian Academy of Sciences, 47 Leninsky prosp., 119991 Moscow, Russian Federation. Fax: +7 (499) 135 5328*

[c] *N. N. Semenov Institute of Chemical Physics, Russian Academy of Sciences, 4 ul. Kosygina, 119991 Moscow, Russian Federation. Fax: +7 (495) 651 2191*

The photochromic ring closure in diarylethylene was studied by femtosecond laser spectroscopy. The absorption spectrum of the initial excited state under pulse excitation at 305 nm was observed. The kinetic scheme of transitions from the initial excited state to the closed-ring isomer as the final product is proposed.

Key words: femtosecond laser spectroscopy, diarylethylenes.

Diarylethylenes are of practical interest as photochromic optical switches highly resistant to thermal and photochemical effects.[1] The design of superfast switching devices based on these compounds is of particular interest. This gave impetus to research on the picosecond and femtosecond dynamics of photochromic ring-closure and ring-opening reactions for selected representatives of diarylethylenes by laser kinetic spectroscopy. In addition, the photochromism of diarylethylenes has attracted attention from researchers as a convenient model system for research on the mechanism of electrocyclic reactions and the application of the Woodward—Hoffmann rules invoking the conservation of orbital symmetry[2] to the one-step mechanism of the closure of the 6π-electron ring *via* the conrotatory path in the excited state.[3]

Previous investigations of the dynamics of the ring closure in diarylethenes have shown that the reaction takes place in the picosecond time scale and is characterized by the complex kinetics.[4—19] In particular, the ring closure of thiophene-based diarylethenes occurs by a one-step mechanism without the formation of intermediates;[4,5] however, in the case of diarylethenes having thiophene oligomers, the intermediate state is observed within 100 fs followed by the ring closure with a characteristic time of 1.1 ps.[6] In more recent studies,[7—9] a short-lived intermediate has been observed in the ring-closure reaction of related thiophene-based diarylethenes. In the study,[13] the pre-switching scheme was proposed as an explanation of the reaction mechanism. This scheme involves the formation of the intermediate state with a fast mixing and relaxation of electronic states in the subpicosecond time scale followed by the ring closure with a characteristic time of 4.2 ps. A similar conclusion was drawn in the study,[15] but a different time separation of the paths was suggested: the fast path occurs within 1—2 ps, whereas the characteristic time of the slow path is approximately several hundred picoseconds,[15] the reaction rate *via* the slow path being dependent on the viscosity of the solvent.[15] Recently, the pathway of the cyclization of diarylethenes through the triplet-excited state has been proposed.[19]

A sufficient time resolution necessary for the measurement of the time of the formation of the first intermediate (approximately 70 fs) was achieved in the study.[9] In the studies,[6—8] the lifetime of the intermediate was estimated with a high error, because the time resolution was not better than 200 fs.

The aim of the present study was to investigate the dynamics of the ring closure in 1-[(4-{5-[4-chloromethyl-2,5-dimethyl-3-thieny]-2-oxo-1,3-dioxol-4-yl}-2,5-dimethyl-3-thienyl)methyl]pyridinium chloride (**1**) by femtosecond laser photolysis under pulse excitation at 305 nm with a duration of 50 fs. Earlier, salt **1** has not been studied by femtosecond laser photolysis. An essential characteristic feature of salt **1** is the presence of the pyridinium

Published in Russian in *Izvestiya Akademii Nauk. Seriya Khimicheskaya,* No. 6, pp. 1093—1102, June, 2011.

1066-5285/11/6006-1118

moiety as the side substituent, resulting in an increase in the solubility of the salt in polar solvents. This is of great interest for practical applications.

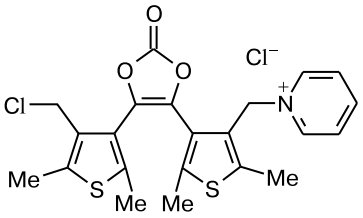

1

Experimental

The ^{1}H NMR spectra were recorded on a Bruker Avance spectrometer (500 MHz) in DMSO-d_6. The mass spectra were obtained on a Kratos MS-30 spectrometer. Dioxolone **2** was synthesized according to a published procedure.[20]

4,5-Bis[4-chloromethyl-2,5-dimethyl-3-thienyl]-1,3-dioxol-2-one (3). A suspension of dioxolone **2** (0.153 g, 0.5 mmol) and paraformaldehyde (0.075 g, 2.5 mmol) in a mixture of concentrated hydrochloric acid (2 mL) and acetic acid (5 mL) was stirred at room temperature for 48 h and then poured into water. The precipitate that formed was filtered off. The yield was 72%, m.p. 119—121 °C. ^{1}H NMR, δ: 1.95 (s, 6 H, 2 Me), 2.40 (s, 6 H, 2 Me), 4.70 (s, 4 H, 2 CH_2). MS, *m/z*: 406, 404, 402 $[M]^+$.

1-[(4-{5-[4-Chloromethyl-2,5-dimethyl-3-thienyl]-2-oxo-1,3-dioxol-4-yl}-2,5-dimethyl-3-thienyl)methyl]pyridinium chloride (1). A solution of dioxolone **3** (0.4 g, 1 mmol) and pyridine (0.08 g, 1 mmol) in acetone (5 mL) was kept at room temperature for 7 days. The precipitate that formed was filtered off and washed on a filter with acetone. The yield was 61%, m.p. 143—145 °C. ^{1}H NMR, δ: 1.95 (s, 3 H, Me); 2.00 (s, 3 H, Me); 2.35 (s, 3 H, Me); 2.50 (s, 3 H, Me); 4.65 (s, 2 H, CH_2); 5.90 (s, 2 H, CH_2); 8.12 (m, 2 H, 2 H_{Py}); 8.61 (m, 1 H, H_{Py}); 8.80 (m, 2 H, 2 H_{Py}).

Steady-state photolysis. Bidistilled ethanol (reagent grade) was used as the solvent. Chloroform (Aldrich, 99% purity) was used without additional purification.

The absorption spectra were recorded on an Ocean Optics HR 2000 spectrometer in the automatic scan mode at specified intervals of time. The irradiation was performed with the use of a PL-S 9W low-pressure mercury-vapor gas-discharge lamp emitting UV radiation in the 340—390 nm range with a maximum at 355 nm.

Femtosecond laser spectroscopy. Induced absorption in solutions of salt **1** was recorded by femtosecond laser absorption spectroscopy using the excitation-probe technique on an instrument described earlier.[21] Femtosecond pulses were generated in a Spectra Physics Tsunami solid-state titanium-doped sapphire laser (τ = 80 fs, E = 0.8 nJ, λ = 802 nm, f = 80 MHz) continuous wave-pumped by a Spectra Physics MilleniaVs solid-state laser with diode pumping (λ = 530 nm, P = 4.65 W). After the enhancement in a Spectra Physics Spitfire regenerative amplifier pumped by a Spectra Physics Evolution X laser (P = 8 W, λ = 527 nm, f = 1 kHz, τ = 150 ns), femtosecond pulses with the parameters τ = 90 fs, E = 1200 μJ, λ = 805 nm, f = 1 kHz were produced.

To generate the excitation and probe pulses, the amplified emission was divided into two beams. One beam designed for the production of excitation pulses was directed to the delay line allowing the delay of the excitation pulse relative to the probe pulse in the range of 0—600 ps with the minimum step of 3.3 fs. The laser pulse was directed thereafter to a Clark MXR NOPA non-collinear optical parametric amplifier, which transformed the 805 nm wavelength into pulses with a wavelength λ = 610 nm, τ = 20 fs. The pulses thus produced were transformed by means of a nonlinear optical crystal into second-harmonic pulses (λ = 305 nm) with an energy of 170 nJ and the duration of 50 fs, and the latter were used for the excitation of a sample.

The second beam of the amplified laser emission was attenuated to an energy of ~0.5—2 μJ and focused onto a cell with water, in which the supercontinuum pulse was generated within the spectral range of 400—1000 nm with a total energy lower than 10 nJ. The supercontinuum pulse was divided into two channels, *viz.*, the probe and reference pulses. The signals were recorded with an Acton SP-300 polychromator and a Princeton Instruments Pixis 100 CCD camera. The induced absorption spectrum was recorded as the differential absorption spectrum in the single-pulse mode.[21,22] For each time delay, the signal was averaged over several hundred pulses. The experimental data were processed with the use of the Matlab program package and the IgorPro software.

The experiments were carried out at room temperature in a flow cell with a 5 mm path length to prevent the accumulation of the closed form of compound **1**. The concentration of the photochrome was $5.04 \cdot 10^{-3}$ and $3.65 \cdot 10^{-3}$ mol L^{-1} in ethanol and chloroform, respectively. In control experiments, the nonlinear optical response of the solvent was measured. In the latter case, the coherent response of nonlinear optical polarization of the solvent typical of femtosecond photolysis was observed. The coherent response signal of the pure solvent was subtracted according to a known procedure[23—25] from the total signal of salt **1** in the solvent and the coherent response of the solvent. The subtraction revealed the signal of **1** in the overlap time window for the excitation and probe pulses (~50 fs).

Results and Discussion

Pyridinium salt **1** was synthesized in two steps (Scheme 1). The key step involves the chloromethylation of dithienylethene **2** (see Ref. 20) giving the corresponding derivative **3**.

Steady-state photolysis. After UV irradiation of solutions of salt **1**, a product showing an absorption band with maxima at 434 and 452 nm in ethanol and chloroform, respectively, was obtained. The product should be assigned to the closed form of photochrome **1** (Scheme 2). After visible-light irradiation (430—470 nm), the spectra restore the initial shape.

Femtosecond photolysis. Figure 1 gives a general view of the dynamics of the induced differential absorption spectra of salt **1** in a subpicosecond time window. As can be seen from Fig. 1, the completion of the excitation pulse was followed by the formation of a broad absorption band in the range from 410 to 700 nm with two pronounced maxima at 550 and 650 nm. The intensity of this absorption band substantially decreases within 300 fs, resulting

Scheme 1

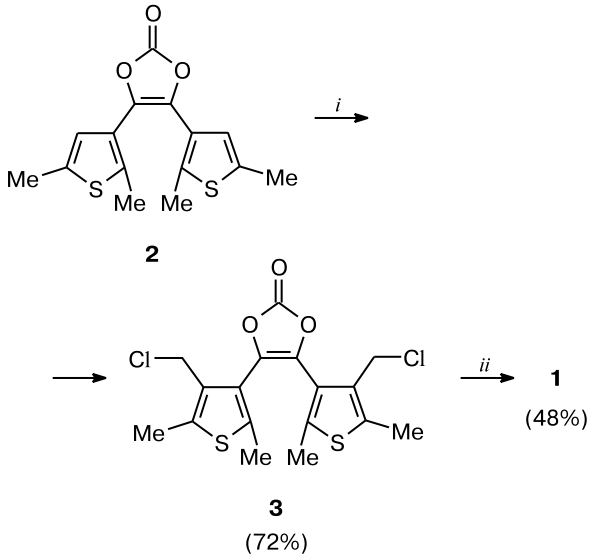

i. $(CH_2O)_n$, HCl, AcOH, 20 °C, 48 h; *ii*. pyridine, acetone, 20 °C, 7 days.

Scheme 2

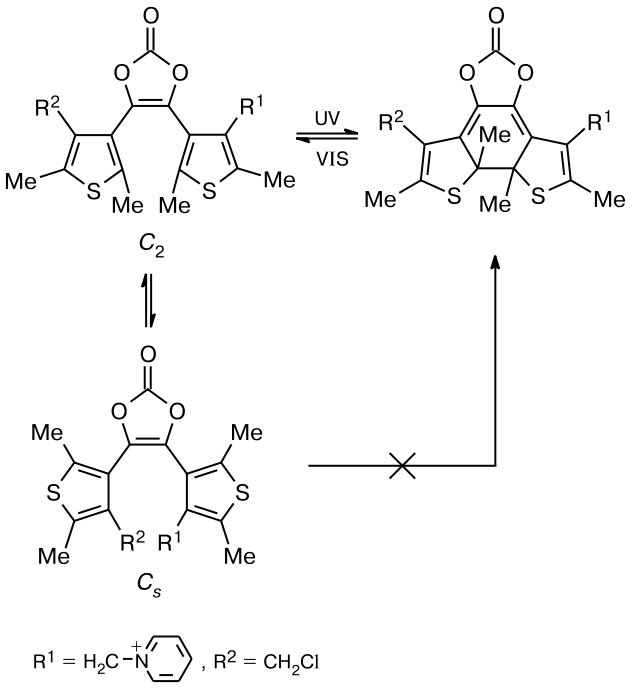

in the formation of a longer-lived absorption band with a maximum at 450 nm, whose intensity remains virtually unchanged in the time window from 1 to 1.5 ps. It is clearly seen that the absorption band with a maximum at 450 nm is formed with a time delay of approximately 200—300 fs.

The changes in the spectra at femtosecond delays are shown in more detail in three time windows. At time delays of 0—60 fs (see Fig. 1, *a*, *d*), the intensity of the broad absorption bands at 544 and 633 nm in ethanol and at 544 and 641 nm in chloroform increases. In the 480—490 nm range, there is an absorption shoulder, which is transformed into a broad absorption band with a maximum at 470 nm in both solvents. The increase in the absorption at time delays from 0 to 60 fs is associated with an increase in the population of the excited state due to the action of the pump pulse (~50 fs). At delay times of 70—170 fs (see Fig. 1, *b*, *e*), the intensity of the band at 500—750 nm with maxima at 544 and 635—641 nm decreases with a simultaneous increase in the maximum at 450 nm. In the time window from 200 fs to 2 ps (see Fig. 1, *c*, *f*), the most substantial changes in the absorption are observed in the range from 200 to 500 fs in the red spectral region. In the time window from 600 fs to 2 ps, the spectrum changes only slightly. The spectra at delay times of 600 and 900 fs are only slightly different and are similar in shape to the spectrum at 2 ps.

The fast changes in the absorption spectra in the time window of up to 600 fs are followed by slow transformations of the spectrum. Figure 2 shows the changes in the spectra from 5 to 500 ps in ethanol and chloroform. The normalized spectra at time delays of 5 and 500 ps are displayed in the insets of Fig. 2, which provides a comparison of the spectral patterns at these time delays. As can be seen from Fig. 2, in ethanol the peak is slightly shifted from 440 nm (2 ps) to 450 nm (500 ps), the half-width remaining virtually unchanged. In ethanol, the intensity of the broad absorption band in the range from 520 to 770 nm is lower compared with the maximum at 450 nm. In chloroform, the spectrum of salt **1** at a time delay of 5 ps is less different from the spectrum at a time delay of 500 ps (see Fig. 2, *b*, the inset), the broad-band shoulder being more pronounced than that in ethanol, and it can be observed at longer time delays (up to 500 ps). An important fact is that the intensity of the absorption spectrum of salt **1** decreases with the change in the time delay from 5 to 500 ps by a factor of more than four for solutions both in ethanol and chloroform. The absorption bands at 440—450 nm in chloroform and ethanol at time delays from 5 to 500 ps are similar in the position and shape to the absorption band of the closed form of **1** (see Fig. 2).

In the analysis of the cyclization reaction, two conformations[12,23,24] shown in Scheme 2 should be considered:

1) the C_2 conformation, which is involved in the fast cyclization reaction and is characterized by a low fluorescence quantum yield;

2) the C_s conformation, for which the cyclization is actually forbidden but which is characterized by a high fluorescence quantum yield.

In the C_s conformer, two methyl groups are oriented in the same direction with respect to the plane of the figure, whereas these groups in the C_2 conformer are oriented in the opposite directions. The symmetry is not exact; as can

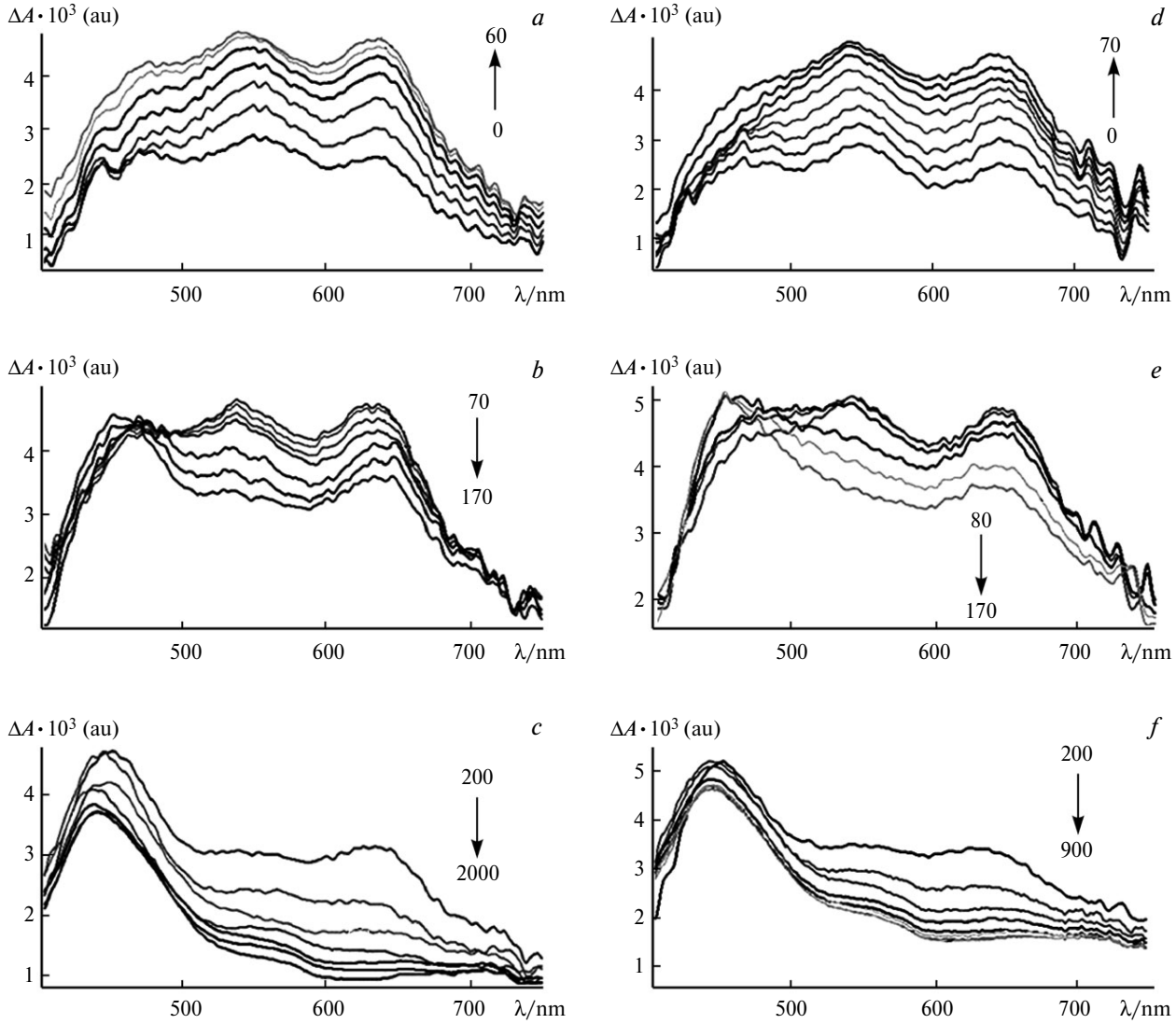

Fig. 1. Dynamics of the absorption spectra of salt **1** in ethanol (*a*—*c*) and chloroform (*d*—*f*). Three time windows in the time range from 0 to 2 ps are shown. The delay times in femtoseconds are: 0, 10, 20, 30, 40, 50, 60 (*a*); 70, 80, 90, 100, 130, 150, 170 (*b*); 200, 300, 400, 500, 600, 900, 2000 (*c*); 0, 10, 20, 30, 40, 50, 60, 70 (*d*); 80, 90, 100, 130, 150, 170 (*e*); 200, 300, 400, 500, 600, 700, 800, 900 (*f*).

be seen from Scheme 2, the symmetry is violated by the side substituents. Nevertheless, it is reasonable to analyze the cyclization in terms of the C_s and C_2 symmetry. In the C_s conformer, the methyl groups create considerable steric hindrance upon the ring closure, whereas the steric hindrance caused by methyl groups is almost absent in the C_2 conformer.

According to the NMR data,[25,26] two conformers of the open form of diarylethenes exist in the concentration ratio of approximately 1 : 1, and they undergo interconversion fast on the NMR time scale. It was reported[23] that the free energy of the C_s conformer is 125 cm^{-1} higher than the free energy of the C_2 conformer, and the $C_s : C_2$ concentration ratio is 1 : 2, which is consistent with the NMR data published earlier.[27] Two open-ring conformers substantially complicate the kinetic analysis of radiationless transitions after the excitation of diarylethene.

The spectrum of the initial state represented by the absorption spectra in the time window from 0 to 60 fs (see Fig. 1, *a*, *d*) in ethanol is almost identical to that in chloroform. The spectra show a broad absorption band with three peaks at 650, 550, and 460 nm, and they substantially differ from those observed earlier.[5,9] In the studies,[5,9] it was noted that the differential absorption spectrum at zero time delay reveals a pronounced peak at 480 nm with a shoulder in the red spectral region, and this spectrum is similar to the spectrum of the excited side groups comprising diarylethene. At 100—200 fs, the initial spectrum measured in the present study is transformed into the spectrum showing an absorption band at 450—460 nm (see

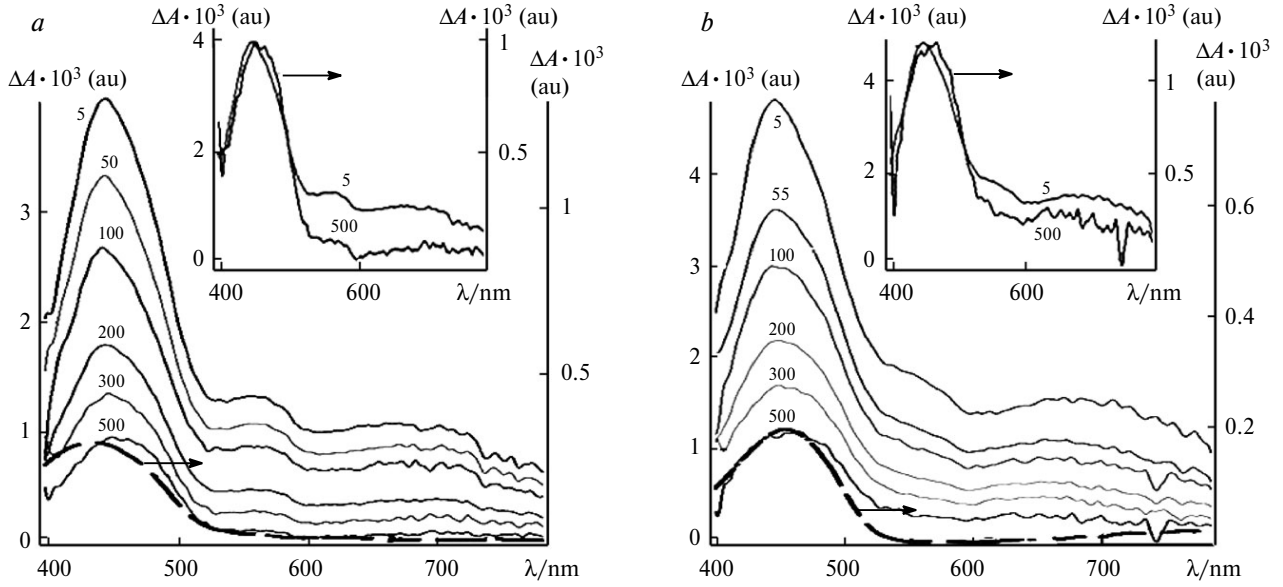

Fig. 2. Absorption spectra of salt **1** in ethanol (*a*) and chloroform (*b*) in the time window from 5 to 500 ps. The absorption spectra of the closed form of **1** measured under steady-state conditions are represented by dashed lines. The insets display the amplitude-normalized spectra in the corresponding solvent at delay times of 5 (*1*) and 500 ps (*2*). The time delays are given in picoseconds.

Fig. 1), whose shape is similar to that recorded in the study.[9] The observed difference in the spectra is apparently attributed to the higher time resolution in the present study, which allowed us to reveal the spectrum of the initial electronic state.

Earlier, it has been noted[9] that the low-lying electron-excited states in the open conformation form nearly degenerate pairs of states with two possible symmetry types A and B, two low electron-excited states being designated as 1B and 2A.[9] The nearly degenerate states 2B and 3A lie ~500 mV higher. The intramolecular motion of the nuclei of diarylethene and the perturbation caused by the solvent molecules leads to the shift of the electronic states A and B and the electron—electron transitions, which can be considered as transitions at points of conical intersections.[28] The fastest transition with a characteristic time of approximately 180 fs should be, apparently, assigned to the transition from the initial electron-excited state to the intermediate electronic state ***P***. As mentioned above, the formation of the intermediate state ***P*** was hypothesized by the authors of the studies;[6—9,13,15] the spectrum of the state ***P*** should be identical to the differential spectrum at a delay time of about 1—2 ps (see Fig. 1, *c*, *f*).

Figure 3 shows the kinetic curves of the changes in the absorption at wavelengths near the absorption maxima. In ethanol, the long-wavelength absorption maxima decay at 640 nm with a constant of 5.1±0.05 ps^{-1} (the characteristic time is 196 fs) and at 550 nm with a constant of 5.2±0.06 ps^{-1} (192 fs). The similar values of the decay constants suggest that both maxima should be assigned to the same intermediate. The kinetic curves at the wavelengths of 450 and 430 nm (see Fig. 3, *c*, *d*) show a rise phase in the initial time region up to 250—300 fs. The approximation of the initial region of the curve by an exponential function gives the time constants of 5.4±0.5 ps^{-1} (185 fs) for 450 nm and 5.2±0.5 ps^{-1} (192 fs) for 430 nm. The fact that the decay constants for the long-wavelength range coincide with the rise constants for the short-wavelength range suggest that the initial state characterized by a broad absorption band with maxima at 480, 545, and 635 nm relaxes to the state with an absorption maximum at 450 nm. A similar decay of the kinetic curves at long wavelengths and the rise in the kinetic curves at short wavelengths are observed in chloroform: the decay constants at 640 and 550 nm are 5.6±0.2 ps^{-1} (182 fs) and 5.4±0.1 ps^{-1} (185 fs), respectively, and the rise constant at 427 nm is 5.6±0.2 ps^{-1} (179 fs). There are some differences in the shape of the kinetic curves for solutions of salt **1** in chloroform and ethanol (*cf.* Fig. 3, *c* and *d*; *d* and *h*). In ethanol, the rise phase in the kinetic curves at the short-wavelength maxima changes for the decay of absorption, which is less pronounced in chloroform.

Noteworthy are the oscillation peaks in the kinetic curves at delay times shorter than ~300 fs, which are particularly pronounced in the initial region of the kinetic curve at 440 nm in ethanol (see Fig. 3, *c* and *d*). In chloroform, oscillation peaks are also observed, but with a lower contrast. The femtosecond pulse coherently excites a superposition of vibrational states of chloroform on the excited-state potential energy surface; a combination of excited vibrational states is referred to as the coherent vibrational wave packet (hereinafter, the wave packet). The oscillation peaks in the kinetic curves are indicative of the appearance of the wave packet; in this case, high-

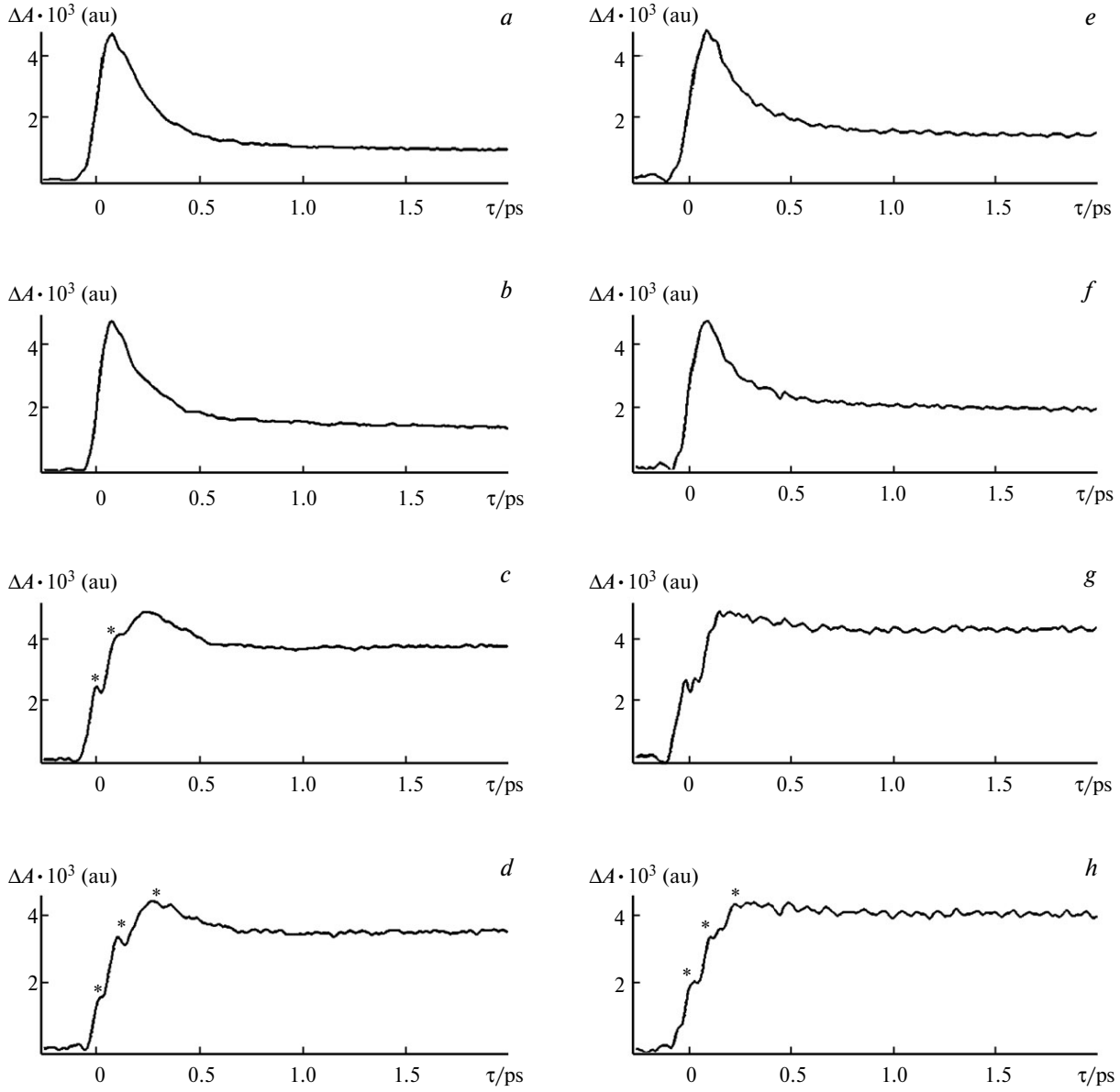

Fig. 3. Kinetic curves of the absorption of salt **1** in ethanol at 640 (*a*), 550 (*b*), 450 (*c*), and 430 nm (*d*) and in chloroform at 640 (*e*), 550 (*f*), 450 (*g*), and 427 nm (*h*). The oscillation peaks are marked with asterisks.

contrast oscillations coupled with the wave packet are observed upon the formation of a primary intermediate. According to the results of the study,[29] oscillations in the kinetic curves should be assigned to the wave packet motion *via* a conical intersection. The observation of oscillations in the rise phase in the kinetic curves upon the formation of the intermediate ***P*** is evidence that the wave packet is observed on the potential energy surface of the state ***P*** and, apparently, the transition *via* the first conical intersection takes place in the coherent regime. The low frequencies 156, 250, and 330 cm^{-1} revealed in the oscillations should be, apparently, attributed to conformational oscillations.

The wave packets quite rapidly decay, as can be seen from the kinetic curves, and this fact is responsible for the broadening of the peaks in the power spectrum (Fig. 4) calculated by the Fourier transform of the kinetic curves shown in Figs 3, *d*, *f*. The dephasing time of the wave packet and the related time of the disappearance of oscillations in the kinetic curve are not longer than 200 fs (see Fig. 3). In ethanol, the oscillations are observed at 156, 250, and 330 cm^{-1}; in chloroform, at 136, 253, and 350 cm^{-1}. The oscillation peaks are virtually identical in ethanol and chloroform and, consequently, the observed oscillations are associated primarily with the intramolecular degrees of freedom and are weakly perturbed by the

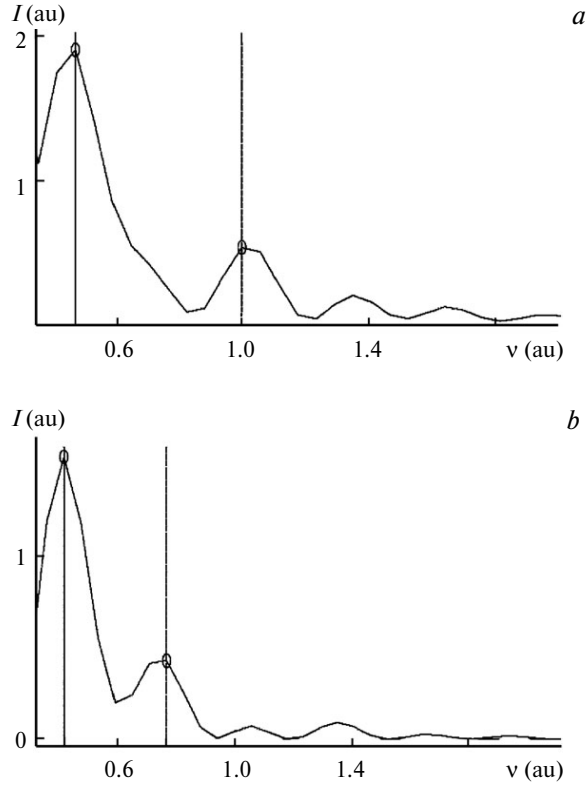

Fig. 4. Power spectra calculated by the Fourier transform of the kinetic curves shown in Figs 3, *d* (*a*) and 3, *h* (*b*). The first two oscillation peaks are marked by vertical lines.

medium. To the best of our knowledge, this is the first observation of the vibrational wave packet in the cyclization reaction of diarylethene. The vibrational wave packet has been observed for the ring opening in 1,2-bis(2-methylbenzo[*b*]thiophen-3-yl)hexafluorocyclopentane.[24]

The intermediate state ***P*** is not the closed-ring reaction product.[9] The transition to this state from the initial electron-excited state may occur in the same way for the C_s and C_2 conformers because the steric repulsion inherent in the C_s conformer should not play a substantial role after the transition to the state ***P***, provided that the ring closure does not occur. Hence, based on the dynamics of the differential spectra (see Fig. 1) and the shape of the kinetic curves (see Fig. 3), it can be hypothesized that both conformers have similar absorption spectra and exhibit similar dynamics of the transition from the initial excited state.

Considerable changes in the differential spectra are observed in the time scale up to 500 ps. Thus, the intensity of the absorption band with a maximum at 450 nm decreases by a factor of more than four (see Fig. 2). The position and the shape of the absorption band for the final reaction product, *viz.*, the closed-ring isomer, prepared under steady-state conditions are similar to those observed in the differential absorption spectrum. The transitions represented as the kinetic curves (Fig. 5) and as the Fourier transform of the spectra (see Fig. 2) reflect the ring closure and the relaxation to the ground state. These processes are shown in Fig. 6 on the condition that the pericyclic ring closure is the major mechanism. In the step of picosecond processes, the dynamics of the state ***P*** for the C_s conformer should be substantially different from that for C_2. Thus, in the case of the C_s conformer, the ring closure in the intermediate state ***P*** does not take place, whereas the conformational transition $C_s \rightarrow C_2$ in the state ***P*** that occurs *via* rotation of the thienyl moieties may play a substantial role in the kinetics of the closed ring formation. This hypothesis is based on the fact that the characteristic times of the process are close to 100 ps. Contrary to the supposition about the characteristic time of the conformational transition in the millisecond scale made in the study,[9] we suggest the possibility of rotation of the side group in the hundred picosecond scale. The time of rotation of the moieties with a relatively small volume, such as the side groups in compound **1**, estimated by the Stokes equation is at most 50 ps. Although this rotation is not completely free, the estimation at 50 ps suggests that this transition could take place. On the condition that the spectrum of the intermediate ***P*** resembles the spectrum of the closed form of compound **1**, a more than a fourfold decrease in the intensity of absorption (see Fig. 2) can be explained, by means of the scheme presented in Fig. 6, as the relaxation to the ground state.

Apparently, the kinetics of the ring closure in all steps of the process, even in the step of femtosecond transformations, is essentially controlled by conformational transitions in the diarylethene molecule, where the solvent plays a substantial role. For example, the shapes of the kinetic curves in ethanol and chloroform at short delay times are somewhat different; at long delay times, they are even approximated by different dependences and are determined by the single- and double-exponential kinetics in ethanol and chloroform, respectively (see Fig. 5). The absorption decay curves in ethanol are well approximated by the single-exponential function (Table 1). In chloroform, the relaxation is slower and the single-exponential function is insufficient for the approximation of the absorption decay curve. The approximation parameters of the decay curves in chloroform by means of the double-exponential function $A = A_1\exp(-k_1t) + A_2\exp(-k_2t)$ are given in Table 1.

The rate constants (see Table 1) in ethanol and chloroform are substantially different, which is in qualitative agreement with the results of the study,[15] where it was found that the viscosity of the solvent has an effect on the kinetics of the cyclization of diarylethene in the picosecond time scale associated with the conformational motion. The conformational transitions necessary for the ring closure and the formation of the σ(C—C) bond require the rotation of the side rings and their close arrangement. In the systems with diarylethenes studied earlier, the steps of

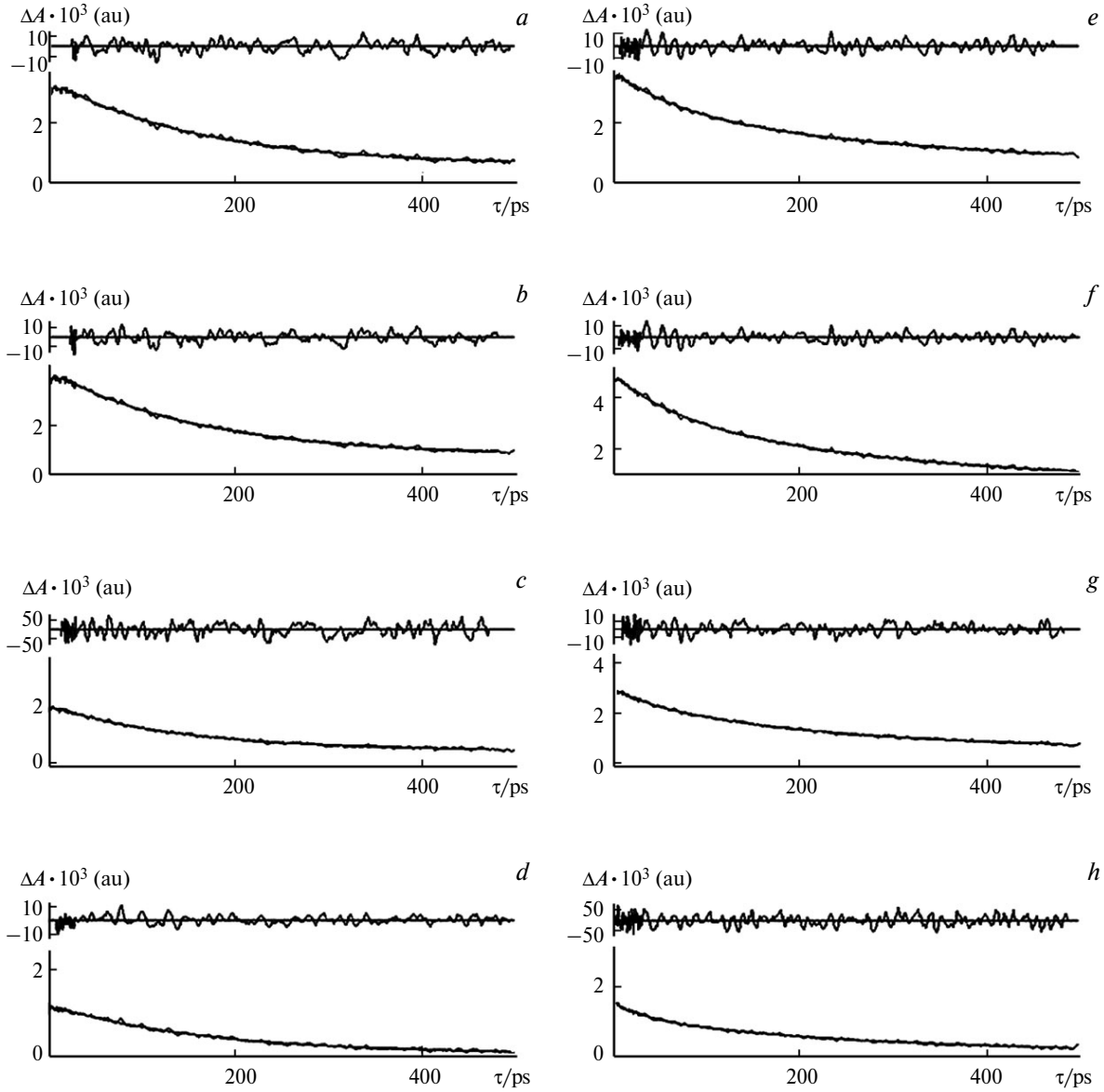

Fig. 5. Kinetics of the absorption relaxation in the time scale from 20 to 500 ps in ethanol at 420 (*a*), 440 (*b*), 500 (*c*), and 700 nm (*d*) and in chloroform at 420 (*e*), 450 (*f*), 500 (*g*), and 700 nm (*h*). The kinetic curves obtained in ethanol were approximated by a single-exponential function; in the case of chloroform, by a double-exponential function. The differential lines calculated by the subtraction of the approximation curves from the experimental data are shown above the kinetic curves.

fast (approximately 100 fs) and slow (approximately 1—10 ps) changes were observed in the absorption spectra. The fast step was assigned to the formation of the primary intermediate, and the slow step was attributed to the ring closure with a characteristic time of 1.1 ps (see Ref. 6) or ~4 ps.[9] Diarylethene **1** under consideration is characterized by slow transitions with a time (see above) of about 285 ps, which is substantially longer than several picoseconds, and it is hardly probable that these transitions are associated with the elementary event of the ring closure. The observed slow processes should be assigned to the conformational motion, which determined the further pathways of the transition from the state ***P***: in the case of the C_s conformer the transition occurs only to the ground state, whereas in the case of the C_2 conformer the transition results in either the products ***C*** or the ground state (see Fig. 6). A deeper insight into this problem can be obtained by performing quantum chemical calculations of the electronic structure and molecular dynamics calculations for compound **1**, which will be the aim of our next study of this system. The convincing evidence for the possibility of the existence of electron-excited diarylethene is the observation of fluorescence that decays with a time constant of 100 ps. This value is of the

Table 1. Approximation parameters of the absorption decay curves for compound **1** in ethanol and chloroform

Solvent	λ/nm	k_1	k_2	A_1/A_2
		ps^{-1}		
Ethanol	420	0.0062	—	—
	440	0.0063	—	—
	500	0.0068	—	—
	700	0.0060	—	—
	420	0.0062	—	—
Chloroform	420	0.016	0.0035	0.47
	440	0.019	0.0040	0.41
	450	0.018	0.0039	0.41
	500	0.033	0.0049	0.22
	700	0.032	0.0041	0.35

same order of magnitude as the constants determined in the study.[24]

Noteworthy is another important fact related to diarylethene **1**. The redox potential of the one-electron reduction of the pyridinium ion $E_{1/2}(A^{-\bullet}/A)$ varies from –500 to –700 mV with respect to the calomel electrode. The potential of the one-electron oxidation of diarylethene $E_{1/2}(D/D^{+\bullet})$ generally varies from 1 to 1.3 eV. The excitation energy of the open form (E^*) is lower than ~3 eV, because the absorption maximum is observed in the region lower than 400 nm. Hence, system **1** can be considered as the covalently linked donor-acceptor pair, where the pyridinium and diarylethene moieties act as the acceptor A and the donor D, respectively. The free energy of the electron transfer from photoexcited diarylethene to pyridinium is determined by the expression $\Delta G \approx E_{1/2}(D/D^{+\bullet}) - E_{1/2}(A^{-\bullet}/A) - E^* + e^2/\varepsilon R$, where ε is the dielectric permeability of the solvent and R is the distance between the donor and the acceptor.[30,31] The value $\Delta G \approx -1$ eV suggests the formation of this charge-transfer state of salt **1**.

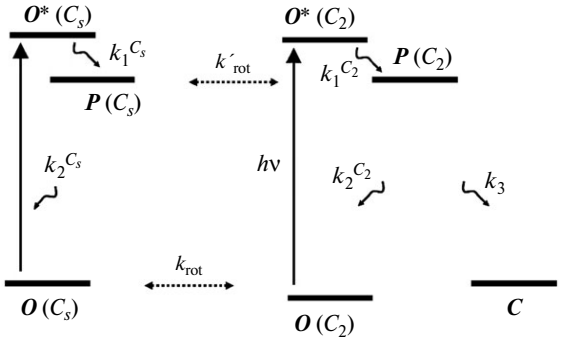

Fig. 6. Radiationless transitions for the C_s and C_2 conformers of compound **1**. ***O*** and ***O**** are the ground and initial photoexcited states, respectively, of the open isomer of diarylethene, ***P*** is the excited state of the ring "pre-closure," and ***C*** is the photoproduct, *viz.*, the closed isomer of diarylethene.

The diarylethene radical cation undergoes cyclization.[32] Hence, in addition to the mechanism shown in Fig. 6, another mechanism of cylclization of compound **1** may be suggested (Scheme 3).

Scheme 3

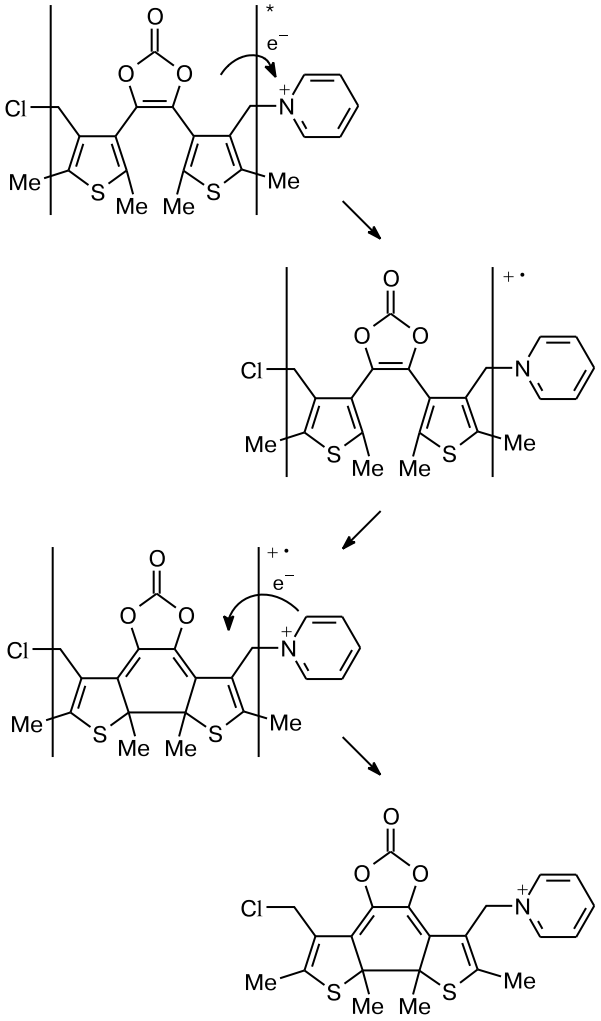

To sum up, we investigated the photochromic ring closure in diarylethene **1** by femtosecond laser spectroscopy. The absorption spectrum of the initial excited state was revealed under pulse excitation at 305 nm. It was shown that the characteristic time of the transition from the initial electron-excited state to the intermediate state is about 180 fs, and the kinetics of this transition is characterized by the coherent wave packets at 156, 250, and 330 cm^{-1}. It was shown that substantial changes in the intermediate spectra occur in the time scale from 2 to 500 ps. The kinetic scheme of transitions from the initial excited state to the closed-ring isomer as the final product was suggested based on the knowledge of the pericyclic closure-ring reaction. It was supposed that the picosecond processes

are controlled by conformational transitions. Based on the thermodynamic estimations, it was hypothesized that diarylethene **1** can undergo cyclization *via* the intramolecular charge-transfer state.

References

1. N. Tamai, H. Miyasaka, *Chem. Rev.*, 2000, **100**, 1875.
2. R. B. Woodward, R. Hoffman, *The Conservation of Orbital Symmetry*, Verlag Chemie, Acad. Press, Weinheim, 1970, 177 pp.
3. S. Nakamura, M. Irie, *J. Org. Chem.*, 1988, **53**, 6136.
4. N. Ohtaka, Y. Hase, K. Uchida, M. Irie, N. Tamai, *Mol. Cryst. Liq. Cryst.*, 2000, **344**, 83.
5. J. C. Owrutsky, H. H. Nelson, A. P. Baronavski, O.-K. Kim, G. M. Tsivgoulis, S. L. Gilat, J.-M. Lehn, *Chem. Phys. Lett.*, 1998, **293**, 555.
6. N. Tamai, T. Saika, T. Shimidzu, M. Irie, *J. Phys. Chem.*, 1996, **100**, 4689.
7. A. T. Bens, J. Ern, K. Kuldova, H. P. Trommsdorff, C. Kryschi, *J. Lumin.*, 2001, **94—95**, 51.
8. J. Ern, A. T. Bens, H.-D. Martin, K. Kuldova, H. P. Trommsdorff, C. Kryschi, *J. Phys. Chem. A*, 2002, **106**, 1654.
9. P. R. Hania, R. Telesca, L. N. Lucas, A. Pugzlys, J. van Esch, B. L. Feringa, J. G. Snijders, K. Duppen, *J. Phys. Chem. A*, 2002, **106**, 1654.
10. P. L. Gentili, E. Danilov, F. Ortica, M. A. Rodgers, G. Favaro, *J. Photochem. Photobiol. Sci.*, 2004, **3**, 886.
11. M. Rini, A. K. Holm, E. T. Nibbering, H. Fidder, *J. Am. Chem. Soc.*, 2003, **125**, 3028.
12. J. Ern, A. Bens, H. D. Martin, S. Mukamel, D. Schmid, S. Tretiak, E. Tsiper, C. Kryschi, *J. Lumin.*, 2000, **87—89**, 742.
13. P. R. Hania, R. Telesca, L. N. Lucas, A. Pugzlys, J. van Esch, B. L. Feringa, J. G. Snijders, K. Duppen, *J. Phys. Chem. A*, 2002, **106**, 8498.
14. P. R. Hania, A. Pugzlys, L. N. Lucas, J. J. D. de Jong, B. L. Feringa, J. van Esch, H. T. Jonkman, K. Duppen, *J. Phys. Chem. A*, 2005, **109**, 9437.
15. H. Miyasaka, T. Nobuto, M. Murakami, A. Itaya, N. Tamai, M. Irie, *J. Phys. Chem. A*, 2002, **106**, 8096.
16. K. Yagi, C. F. Soong, M. Irie, *J. Org. Chem.*, 2001, **66**, 5419.
17. H. Tamura, S. Nanbu, T. Ishida, H. Nakamura, *J. Chem. Phys.*, 2006, **124**, 084313.
18. C. Okabe, T. Nakabayashi, N. Nishi, T. Fukaminato, T. Kawai, M. Irie, H. Sekiya, *J. Phys. Chem. A*, 2003, **107**, 5384.
19. M. T. Indelli, S. Carli, M. Ghirotti, C. Chiorboli, M. Ravaglia, M. Garavelli, F. Scandola, *J. Am. Chem. Soc.*, 2008, **130**, 7286.
20. M. M. Krayushkin, S. N. Ivanov, A. Yu. Martynkin, B. V. Lichitskii, A. A. Dudinov, L. G. Vorontsova, Z. A. Starikova, B. M. Uzhinov, *Izv. Akad. Nauk, Ser. Khim.*, 2002, 1588 [*Russ. Chem. Bull., Int. Ed.*, 2002, **51**, 1731].
21. I. V. Shelaev, F. E. Gostev, V. A. Nadtochenko, A. Ya. Shkuropatov, A. A. Zabelin, M. D. Mamedov, A. Yu. Semenov, O. M. Sarkisov, V. A. Shuvalov, *Photosynth. Res.*, 2008, **98**, 95.
22. S. A. Kovalenko, R. Schanz, V. M. Farztdinov, H. Hennig, N. P. Ernsting, *Chem. Phys. Lett.*, 2000, **323**, 312.
23. S. Shim, I. Eom, T. Joo, E. Kim, K. S. Kim, *J. Phys. Chem. A*, 2007, **111**, 8910.
24. S. Shim, T. Joo, S. C. Bae, K. S. Kim, E. Kim, *J. Phys. Chem. A*, 2003, **107**, 8106.
25. K. Uchida, Y. Nakayama, M. Irie, *Bull. Chem. Soc. Jpn.*, 1990, **63**, 1311.
26. M. Irie, K. Sakemura, M. Okinaka, K. Uchida, *J. Org. Chem.*, 1995, **60**, 8305.
27. K. Uchida, E. Tsuchida, Y. Aoi, S. Nakamura, M. Irie, *Chem.Lett.*, 1999, 63.
28. M. Klessinger, *Angew. Chem., Int. Ed.*, 1995, **34**, 549.
29. G. A. Worth, L. S. Cederbaum, *Annu. Rev. Phys. Chem.*, 2004, **55**, 127.
30. I. V. Rubtsov, D. V. Khudiakov, A. P. Moravskii, V. A. Nadtochenko, *Chem. Phys. Lett.*, 1996, **249**, 101.
31. V. A. Nadtochenko, N. N. Denisov, P. P. Levin, *Izv. Akad. Nauk, Ser. Khim.*, 1995, 1078 [*Russ. Chem. Bull.* (*Engl. Transl.*), 1995, **44**, 1038].
32. G. Guirado, Ch. Coudret, M. Hliwa, J.-P. Launay, *J. Phys. Chem. B*, 2005, **109**, 17445.

Received March 4, 2011;
in revised form May 19, 2011